

Demonstration of quasi-monoenergetic electron-beam generation in laser-driven plasma acceleration

Eisuke Miura,^{a)} Kazuyoshi Koyama, Susumu Kato, and Naoaki Saito

National Institute of Advanced Industrial Science and Technology (AIST), Tsukuba Central 2, 1-1-1 Umezono, Tsukuba, Ibaraki 305-8568, Japan

Masahiro Adachi

Hiroshima University, 1-3-1 Kagamiyama, Higashi-Hiroshima, Hiroshima 739-8530, Japan

Yoichi Kawada

University of Tsukuba, 1-1-1 Tennodai, Tsukuba, Ibaraki 305-8577, Japan

Tatsufumi Nakamura^{b)}

National Institute of Radiological Sciences, 4-9-1 Anagawa, Inage, Chiba, Chiba 263-8555, Japan

Mitsumori Tanimoto

Meisei University, 2-1-1 Hodokubo, Hino, Tokyo 191-8506, Japan

(Received 24 May 2004; accepted 11 May 2005; published online 14 June 2005)

The generation of a quasi-monoenergetic electron beam in laser-driven plasma acceleration is reported. A monoenergetic electron beam with an energy of 7 MeV was emitted from a high-density plasma (electron density $>10^{20}$ cm⁻³) produced by a 2 TW 50 fs laser pulse. The divergence of the monoenergetic beam was $\pm 1.2^\circ$. The first Stokes satellite peak of stimulated forward Raman scattering was observed in the spectrum of the light transmitted through the plasma. The plasma wave was excited in the region of which electron density was around 1.3×10^{20} cm⁻³. The acceleration length was estimated to be 500 μ m from the length of the side-scattered light image. It is considered that the monoenergetic beam generation is due to the matching of the acceleration length to the dephasing length determined by the velocity difference between the accelerated electrons and the plasma wave. © 2005 American Institute of Physics. [DOI: 10.1063/1.1949289]

Particle acceleration via the interaction of an intense laser pulse with a plasma has been intensively studied to realize an advanced compact accelerator¹ since the fundamental concept was proposed.² An electron beam with the maximum energy of up to 200 MeV has been obtained using a high-repetition-rate laser system.³ However, the observed energy spectra of accelerated electrons have so far been Boltzmann-type or power-law distributions, and the energy spreads have been large. The key issue in realizing an advanced compact accelerator based on laser-driven plasma acceleration is the generation of a monoenergetic electron beam. It has been reported that a peak was observed in the energy spectrum of accelerated electrons from a low-density (electron density $n_e \sim 10^{16}$ cm⁻³) plasma produced inside a 1 cm long capillary.⁴ On the other hand, it has been also reported that peaks between 6 and 15 MeV were observed in the energy spectra of accelerated electrons from a high-density ($n_e \sim 10^{20}$ cm⁻³) plasma.⁵ The peak formation in the electron energy spectrum suggests that electrons trapped and accelerated in a plasma wave enter the deceleration phase. To realize such a condition, the plasma wave should be excited beyond the dephasing length, which is determined by the velocity difference between the accelerated electrons and the plasma wave. In the linear regime, the dephasing length L_d is given by $L_d \sim \gamma_p^2 \lambda_p$. Here, γ_p and λ_p are the Lorentz factor for the phase velocity of the plasma wave and the wavelength of the plasma wave, respectively. For a low-density

plasma, it is necessary to use a capillary, as shown in Ref. 4, in order to make the plasma length longer, because the dephasing length is the order of centimeter. As the electron density becomes higher, the dephasing length becomes shorter. The dephasing length in the linear regime is estimated to be 58 μ m at the electron density of 10^{20} cm⁻³ for 800 nm laser light. Such short plasma length can be achieved in a gas jet. However, the excitation of a plasma wave has not been observed in a high-density ($n_e \sim 10^{20}$ cm⁻³) plasma, although the generation of a multi-MeV electron beam has been observed.^{6,7} It has been considered that the dominant acceleration mechanism is direct laser acceleration⁸ or stochastic acceleration.⁹ In contrast, the peak formation in the electron energy spectrum reported in Ref. 5 suggests the electron acceleration via the plasma wave as well as the possibility of monoenergetic beam generation in a high-density plasma.

In this letter, we report the demonstration of quasi-monoenergetic electron-beam generation in laser-driven plasma acceleration as well as the evidence of the excitation of a plasma wave. A monoenergetic electron beam with an energy of 7 MeV was emitted from a plasma ($n_e > 10^{20}$ cm⁻³) produced by a 2 TW Ti:Sapphire laser pulse. We observed the excitation of a plasma wave by the measurement of the spectrum of the light transmitted through the plasma and the side-scattered light image.

Figure 1 shows the experimental setup. The experiment was performed with a Ti:Sapphire laser system which delivered a 100 mJ pulse with 50 fs duration. The center wavelength was 800 nm. The 50 mm diameter beam was focused on a supersonic gas jet using an off-axis parabolic mirror

^{a)}Electronic mail: e-miura@aist.go.jp

^{b)}Present address: Institute of Laser Engineering, Osaka University, 2-6 Yamadaoka, Suita, Osaka 565-0781, Japan.

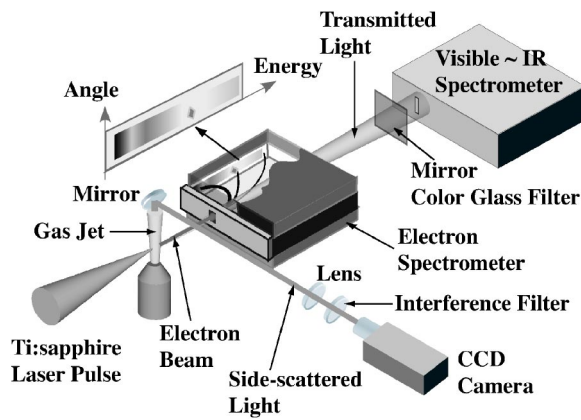


FIG. 1. Experimental setup.

with the focal length of 165 mm. The spot diameter was $5 \mu\text{m}$ at the full width at half maximum. The laser intensity was estimated to be $5 \times 10^{18} \text{ W/cm}^2$ corresponding to the normalized vector potential $a_0 = 1.5$. The contrast ratio of the prepulse, which preceded the main pulse by 5 ns, was 10^{-4} . A nitrogen gas jet was ejected from a supersonic nozzle attached to a pulsed gas valve (General Valve: Series 9). The exit diameter of the nozzle was 1.1 mm. The focal point was set at 1 mm above the nozzle exit. The density profile of the gas jet was measured with a Jamin interferometer. The molecular density at the nozzle center at 1 mm above the nozzle exit was $1.5 \times 10^{19} \text{ cm}^{-3}$, when the filling pressure of the pulsed valve was 30 bar. The barrier suppression ionization model¹⁰ predicts stable ionization to N^{5+} under the laser intensity of our experiment. The electron density at the nozzle center was estimated to be $1.5 \times 10^{20} \text{ cm}^{-3}$. An energy spectrum of accelerated electrons was measured using an electron spectrometer with a permanent magnet. The measured energy range was from 0.2 to 30 MeV. A slit was set in the front of the magnet. The angular divergence was obtained for an electron beam with small divergence. The acceptance angle at 7 MeV was 4.6° . The electron energy spectrum was recorded on an imaging plate [(IP) Fuji Film: BAS-SR]. To prevent exposure by scattered laser light, the IP was covered with $15 \mu\text{m}$ thick Al foil. The sensitivity curve of the IP reported in Ref. 11 was used. To investigate the acceleration mechanism experimentally, we observed the spectrum of the light transmitted through the plasma and the side-scattered light image simultaneously with the electron-beam measurement. A spectrum of light transmitted through a plasma was observed through the hole on the rear side of the electron spectrometer. The observed spectral range was from 650 to 1200 nm. The side-scattered light image was observed through an interference filter of 800 nm.

Figure 2(a) shows an energy-resolved electron image recorded on the IP. The image was obtained by the accumulation of 90 laser shots. The small spot around 7 MeV indicates the generation of a monoenergetic beam with small divergence. Figure 2(b) shows the electron energy spectrum obtained as the average of the 90 shots from the spatially integrated image shown in Fig. 2(a). The number of electrons of the monoenergetic beam was 2.7×10^4 per shot. The energy spread was 20%. The observed energy spread was determined by the low energy resolution of the electron spectrometer. The monoenergetic beam may have much narrower energy spread. The beam divergence of the monoenergetic beam was estimated to be $\pm 1.2^\circ$ from the transverse size of the electron image. The normalized emittance ε_n is given by $\varepsilon_n = \gamma \sigma \delta \theta$. Here, γ , σ , and $\delta \theta$ are the relativistic Lorentz factor for electron energy, the radius of the electron source, and the angular divergence at the half width at half maximum, respectively. Assuming that the electron source radius is $2.5 \mu\text{m}$ which is comparable to the laser spot radius, the normalized emittance is estimated to be $0.7\pi \text{ mm mrad}$. Another small peak at 11 MeV was seen in Fig. 2(b). Our previous result⁵ showed that peaks were formed at different energies, even though the laser energy, the pulse duration, the focal position, and the fulling pressure of the pulsed valve were fixed. Then, it is supposed that in some of 90 shots, the peak at 11 MeV was formed due to the shot-to-shot variation of the laser and/or gas jet conditions. As seen in Fig. 2(a), the divergence ($\pm 0.4^\circ$) of the 11 MeV beam was smaller than that of the 7 MeV beam. The beam divergence can be smaller for the higher-energy electrons, because the relative transverse momentum becomes smaller due to the longer acceleration length or the higher acceleration field. Similar results have been reported.^{3,6} Taking into account of the shot-to-shot variation in 90 shots, it is noted that the number of electrons is the lower limit and the beam divergence is the upper limit.

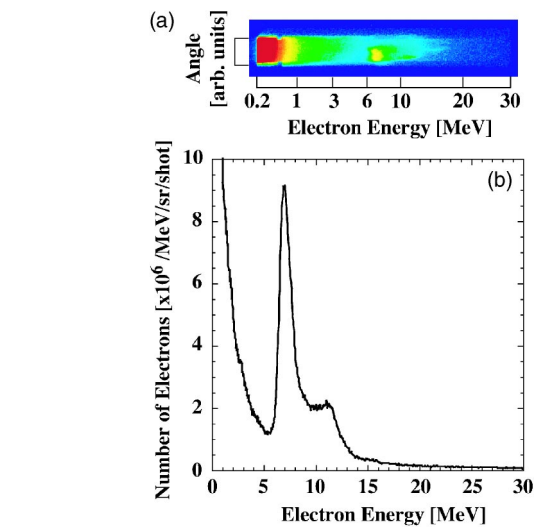


FIG. 2. (Color online) (a) Energy-resolved electron image obtained by the accumulation of 90 laser shots. The small spot around 7 MeV indicates the generation of a monoenergetic beam with small divergence. (b) Electron energy spectrum obtained as the average of 90 shots.

beam was estimated to be $\pm 1.2^\circ$ from the transverse size of the electron image. The normalized emittance ε_n is given by $\varepsilon_n = \gamma \sigma \delta \theta$. Here, γ , σ , and $\delta \theta$ are the relativistic Lorentz factor for electron energy, the radius of the electron source, and the angular divergence at the half width at half maximum, respectively. Assuming that the electron source radius is $2.5 \mu\text{m}$ which is comparable to the laser spot radius, the normalized emittance is estimated to be $0.7\pi \text{ mm mrad}$. Another small peak at 11 MeV was seen in Fig. 2(b). Our previous result⁵ showed that peaks were formed at different energies, even though the laser energy, the pulse duration, the focal position, and the fulling pressure of the pulsed valve were fixed. Then, it is supposed that in some of 90 shots, the peak at 11 MeV was formed due to the shot-to-shot variation of the laser and/or gas jet conditions. As seen in Fig. 2(a), the divergence ($\pm 0.4^\circ$) of the 11 MeV beam was smaller than that of the 7 MeV beam. The beam divergence can be smaller for the higher-energy electrons, because the relative transverse momentum becomes smaller due to the longer acceleration length or the higher acceleration field. Similar results have been reported.^{3,6} Taking into account of the shot-to-shot variation in 90 shots, it is noted that the number of electrons is the lower limit and the beam divergence is the upper limit.

Figure 3(a) shows a typical spectrum of light transmitted through a plasma, when the monoenergetic beam was emitted. It is noted that the incident laser light around 800 nm was attenuated by a multilayer mirror of 800 nm. The part around 700 nm was the component of the ionization blueshift. The first Stokes satellite peak of stimulated Raman forward scattering was observed at 1030 nm. The electron density of the region, in which the plasma wave is excited, can be estimated from the wavelength of the satellite peak. Taking account of the relativistic effect for $a_0 = 1.5$, the electron density was estimated to be $1.3 \times 10^{20} \text{ cm}^{-3}$. Figure 3(b) shows a typical side-scattered light image. The laser light propagated from left to right. The dotted circle shows the position of the nozzle exit. The arrow shows the polarization direction of the incident laser light. When the monoenergetic beam was emitted, the strong side-scattered light image with

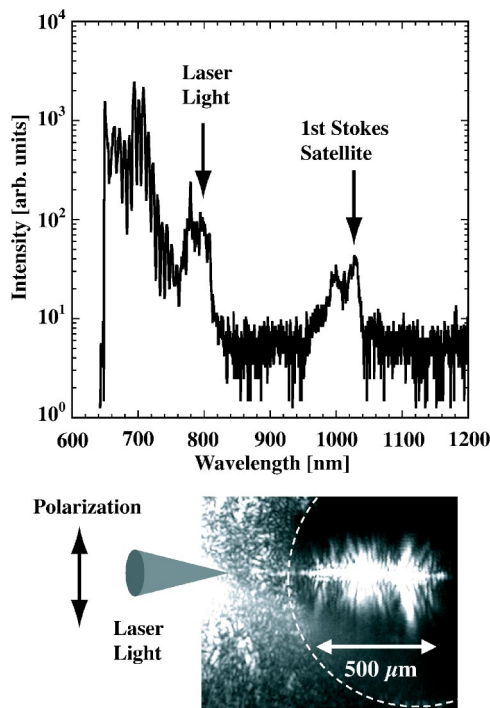


FIG. 3. (a) Spectrum of the light transmitted through the plasma, when the monoenergetic beam was emitted. The first Stokes satellite peak of stimulated forward Raman scattering was observed at 1030 nm. (b) Side-scattered light image observed through an interference filter of 800 nm when the monoenergetic beam was emitted. The polarization direction of the side-scattered light was the same as that of the incident laser light.

a fish-bone structure was observed around the nozzle center. The wavelength of the side-scattered light is similar to that of the incident laser light, because the image was observed through an interference filter of 800 nm. In addition, the polarization direction of the side-scattered light is the same as that of the incident laser light. It is supposed that the side-scattered light is due to coherent Thomson scattering induced by the excitation of a plasma wave.¹² The electron density of the region, in which the side-scattered light was emitted, was estimated to be $(1.0\text{--}1.5) \times 10^{20} \text{ cm}^{-3}$ from the density profile of the gas jet. The electron density fairly agreed with the electron density ($1.3 \times 10^{20} \text{ cm}^{-3}$) estimated from the wavelength of the Stokes satellite. Then, it is reasonable to infer that the plasma wave was excited in the region where the side-scattered light was emitted. From the length of the image, the length of the region where the plasma wave was excited, that is the acceleration length, can be estimated to be $500 \mu\text{m}$.

Here, we discuss the mechanism of the monoenergetic electron-beam generation. When the electron density is $1.3 \times 10^{20} \text{ cm}^{-3}$, the dephasing length is estimated to be $68 \mu\text{m}$ by taking account of the relativistic effect for $a_0 = 1.5$. The dephasing length is much shorter than the acceleration length

of $500 \mu\text{m}$. In such case, the acceleration and the deceleration can be repeated. The acceleration length is nearly equal to seven times the dephasing length. This is equivalent to the case where the acceleration length is nearly equal to the dephasing length. Under such a condition, the self-bunching of electrons entering the deceleration phase can form the monoenergetic peak. It is considered that the monoenergetic electron beam generation was due to the matching of the acceleration length to the dephasing length.

In summary, a monoenergetic electron beam with an energy of 7 MeV was emitted from a plasma ($n_e > 10^{20} \text{ cm}^{-3}$) produced by a 2 TW 50 fs laser pulse. The divergence of the monoenergetic beam was $\pm 1.2^\circ$. A plasma wave was excited in the region of which electron density was around $1.3 \times 10^{20} \text{ cm}^{-3}$. The acceleration length was estimated to be $500 \mu\text{m}$ from the side-scattered light image. The generation of the monoenergetic beam was due to the matching of the acceleration length to the dephasing length. The quasi-monoenergetic electron beam generation will give us a breakthrough to achieve an advanced compact accelerator based on laser-driven plasma acceleration.

A part of this study was financially supported by the Budget for Nuclear Research of the Ministry of Education, Culture, Sports, Science, and Technology (MEXT), based on the screening and counseling by the Atomic Energy Commission, and the Advanced Compact Accelerator Development of the MEXT.

¹D. Umstadter, *J. Phys. D* **36**, R151(2003); R. Bingham, J. T. Mendonça, and P. K. Shukla, *Plasma Phys. Controlled Fusion* **46**, R1 (2004), and references therein.

²T. Tajima and J. M. Dawson, *Phys. Rev. Lett.* **43**, 267 (1979).

³V. Malka, S. Fritzler, E. Lefebvre, M. M. Aleonard, F. Burgy, J. P. Chambaret, J. F. Chemin, K. Krushelnick, G. Malka, S. P. D. Mangles, Z. Najmudon, M. Pittman, J. P. Rousseau, J. N. Scheurer, B. Walton, and A. E. Dangor, *Science* **298**, 1596 (2002).

⁴Y. Kitagawa, Y. Sentoku, S. Akamatsu, W. Sakamoto, R. Kodama, K. A. Tanaka, K. Azumi, T. Norimatsu, T. Matsuoka, H. Fujita, and H. Yoshida, *Phys. Rev. Lett.* **92**, 205002 (2004).

⁵K. Koyama, E. Miura, S. Kato, N. Saito, M. Adachi, Y. Kawada, T. Nakamura, and M. Tanimoto, *Bull. Am. Phys. Soc.* **48**, 350 (2003).

⁶C. Gahn, G. D. Tsakiris, A. Pukhov, J. Meyer-ter-Vehn, G. Pretzler, P. Thirolf, D. Habs, and K. J. Witte, *Phys. Rev. Lett.* **83**, 4772 (1999).

⁷K. Koyama, H. Hazama, N. Saito, and M. Tanimoto, *Int. J. Appl. Electromagn. Mech.* **14**, 263 (2001/2002).

⁸A. Pukhov, Z. M. Sheng, and J. Meyer-ter-Vehn, *Phys. Plasmas* **6**, 2847 (1999).

⁹M. Tanimoto, S. Kato, E. Miura, N. Saito, K. Koyama, and J. Koga, *Phys. Rev. E* **68**, 026401 (2003).

¹⁰S. Augst, D. Strickland, D. D. Meyerhofer, S. L. Chin, and J. H. Eberly, *Phys. Rev. Lett.* **63**, 2212 (1989).

¹¹T. Takahashi, T. Satoh, T. Yabuuchi, R. Kodama, Y. Kitagawa, T. Ikeda, Y. Honda, S. Okuda, and K. A. Tanaka, *Hoshasen* **28**, 203 (2002), in Japanese.

¹²S.-Y. Chen, M. Krishnan, A. Maksimchuk, and D. Umstadter, *Phys. Plasmas* **7**, 403 (2000).